González-Rodríguez, Pedro; Ilan, Boaz; Kim, Arnold D., … et al. (2016) One-way radiative transfer. *Journal of Quantitative Spectroscopy and Radiative Transfer*, v. 176, pp.: 122-128.

DOI: https://doi.org/10.1016/j.jqsrt.2016.02.032

The one-way radiative transfer equation

Pedro González-Rodríguez,[1] Boaz Ilan,[2] and Arnold D. Kim[2]

[1] *Gregorio Millán Institute, Universidad Carlos III de Madrid, Leganés 28911, Spain*
[2] *Applied Mathematics Unit, School of Natural Sciences, University of California, Merced, 5200 North Lake Road, Merced, California, 95343, USA*

We introduce the one-way radiative transfer equation to compute the transmission of a beam incident normally on a slab composed of a uniform forward-peaked scattering medium. As opposed to the radiative transfer equation which must be formulated as a boundary value problem, the one-way radiative transfer equation is formulated as a much simpler initial value problem. We validate the one-way radiative transfer equation through comparisons with Monte Carlo simulations over a broad range of albedo, anisotropy factor, and optical thickness values.

PACS numbers: 030.5620 290.4210, 290.7050, 000.3860

I. INTRODUCTION

Radiative transfer governs the propagation of light in a multiple scattering medium [1, 2]. One particularly important problem in radiative transfer is determining the transmission of a collimated beam incident normally on a plane-parallel, turbid slab. This problem has important applications in atmospheric and ocean optics [3, 4], and biomedical optics [5], among others. This problem remains a challenge because the governing boundary value problem for the radiative transfer equation (RTE) is difficul to solve. For this reason, developing accurate approximations that are easier to solve is useful.

The diffusion approximation applies when the scattering medium is optically thick [2]. This approximation leads to a boundary value problem for the diffusion equation which is a linear, elliptic partial differential equation. The diffusion equation is significantl simpler than the RTE. For this reason, the diffusion approximation has been used extensively, especially for biomedical optics problems. However, the diffusion approximation is only valid for very optically thick media. Even for sufficientl optically thick media, the diffusion approximation suffers from large errors near sources and boundaries. To address the errors made by the diffusion approximation near sources, Vitkin *et al.* [13] introduced the so-called phase function corrected diffusion approximation. By decomposing the scattering phase function into three terms: a delta function, an isotropic part, and an ansitropic part, Vitkin *et al.* derive an additive correction to the diffuse reflectanc that improves the accuracy near the point-of-entry. Alternatively, one can correct the errors made by the diffusion approximation near sources and boundaries using boundary layer analysis [12]. However, this formal and systematic analysis necessarily adds some complexity back into the problem. Regardless, the diffusion approximation is limited only to optically thick media.

Another prominent feature that clouds, oceans and biological tissues often exhibit is forward-peaked scattering. In that case, most of the power scattered by the medium fl ws in the same direction as it is incident. Forward-peaked scattering is challenging computationally because it requires extensive resources to adequately resolve the sharp peak in the scattering phase function. The asymptotic limit of sharply forward-peaked scattering has been studied extensively leading to the Fokker-Planck approximation [6, 7] and its generalizations [8–11]. All of these approximations help to relieve the computational demands of forward-peaked scattering. Nonetheless, each of these approximations leads to the same kind of boundary value problem as the one for the RTE and so each still is a relatively complicated problem to solve. Moreover, these approximations are derived for the extreme case of sharply peaked forward scattering. Rather than being broadly applicable, the accuracy of these models tends to be case-dependent.

Despite the fact that there exists several models to study light propagation in scattering media, there remains a need for new models. Ideally, a new model is conceptually simple, accurate across a broad range of optical parameters, easy to solve, and physically intuitive and insightful. To address this need, we introduce here the one-way RTE. The one-way RTE is derived by restricting the limits of integration in the scattering operator of the RTE to the hemisphere of directions aligned with the incident direction of the collimated beam. This approximation therefore neglects the power scattered by the medium in the opposite hemisphere of directions. Consequently, the one-way RTE leads to a simpler *initial value problem* that can be solved readily. We solve the initial value problem for the one-way RTE to study the transmission of a beam in a slab composed of a uniform scattering and absorbing medium. Through comparisons with Monte Carlo simulations for the full RTE, we show that the one-way RTE provides an accurate and efficaciou approximation for modeling the transmission of beams by a forward-peaked turbid medium across a broad range of optical parameters.

The remainder of this paper is as follows. In Section 2 we discuss the RTE and the boundary value problem for the RTE that governs a beam incident normally on a slab. We consider here the general case in which the refractive index within the slab is different from that outside of the slab. In Section 3 we derive the one-way RTE and the initial value problem for the one-way RTE for beam transmission through a slab. In Section 4 we describe a numerical method to solve the initial value problem for the one-way RTE. We give several numerical results in Section 5 that compare Monte Carlo simulation results with those from the one-way RTE over a broad range of optical parameters. In Section 6 we give our conclusions.

II. THE RADIATIVE TRANSFER EQUATION

Let I denote the intensity that depends on direction, $\hat{\mathbf{s}}$, a vector on the unit sphere, $\mathbb{S}^2$, and position $\mathbf{r}$. In a multiple scattering medium, I is governed by the RTE,

$$\hat{\mathbf{s}}\cdot\nabla I + I = \varpi_0 \int_{\mathbb{S}^2} p(\hat{\mathbf{s}}\cdot\hat{\mathbf{s}}')I(\hat{\mathbf{s}}',\mathbf{r})\mathrm{d}\hat{\mathbf{s}}', \tag{II.1}$$

where ϖ_0 is the single scattering albedo. The spatial variables in Eq. (II.1) are nondimensionalized according to $\mathbf{r} \leftarrow (\mu_a+\mu_s)\mathbf{r}$ with μ_a denoting the absorption coefficient and μ_s denoting the scattering coefficient The scattering phase function p gives the fraction of light scattered in direction $\hat{\mathbf{s}}$ due to light incident in direction $\hat{\mathbf{s}}'$. Here, we use the Henyey-Greenstein scattering phase function define as

$$p(\hat{\mathbf{s}}\cdot\hat{\mathbf{s}}') = \frac{1}{4\pi}\frac{1-g^2}{(1+g^2-2g\hat{\mathbf{s}}\cdot\hat{\mathbf{s}}')^{3/2}}, \tag{II.2}$$

with g denoting the anisotropy factor. In particular, the limit, $g \to 1$, corresponds to scattering only in the forward direction. The scattering phase function p is normalized according to

$$\int_{\mathbb{S}^2} p(\hat{\mathbf{s}}\cdot\hat{\mathbf{s}}')\mathrm{d}\hat{\mathbf{s}}' = 1. \tag{II.3}$$

We are interested in studying the transmission of a Gaussian beam incident normally on the slab, $0 < z < z_0$, composed of a uniform absorbing and scattering medium. The refractive index inside the slab is different from medium on either side of the slab. For that reason, we must take into account partial reflection at the boundaries due to this refractive index mismatch. For this problem we seek the solution of Eq. (II.1) in $0 < z < z_0$ subject to the following boundary conditions.

The collimated beam is incident on $z = 0$, and the associated boundary condition is

$$I(\hat{\mathbf{s}},x,y,0) = t_1(\hat{z})\delta(\hat{\mathbf{s}}-\hat{z})b(x,y) + r_1(\hat{\mathbf{s}}_1\to\hat{\mathbf{s}})I(\hat{\mathbf{s}}_1,x,y,0) \quad \text{on } \hat{\mathbf{s}}\cdot\hat{z}>0, \tag{II.4}$$

with

$$b(x,y) = \frac{2P_0}{\pi R^2}\exp\left[-2\left(x^2+y^2\right)/R^2\right]. \tag{II.5}$$

The firs term in boundary condition (II.4) gives the Gaussian beam define in Eq. (II.5) incident normally on and transmitted across the boundary $z = 0$. Here, $t_1(\hat{z})$ denotes the Fresnel transmission coefficien for light incident on the boundary from outside of the slab in diretion $\hat{z}$. The total power of the beam is denoted by P_0, and the $1/e^2$ radius of the beam is denoted by R. The second term in boundary condition (II.4) gives the reflectio of light incident on the $z = 0$ boundary from within the slab in direction $\hat{\mathbf{s}}_1$ with $\hat{\mathbf{s}}_1\cdot\hat{z} < 0$ and reflecte in direction $\hat{\mathbf{s}}$ as governed by Snell's law. Here, $r_1(\hat{\mathbf{s}}_2\to\hat{\mathbf{s}})$ denotes the Fresnel reflectio coefficien for light incident on the boundary from within the slab.

There is no incident radiation on $z = z_0$ from outside of the slab, so the boundary condition on $z = z_0$ is

$$I(\hat{\mathbf{s}},x,y,z_0) = r_2(\hat{\mathbf{s}}_2\to\hat{\mathbf{s}})I(\hat{\mathbf{s}}_2,x,y,z_0) \quad \text{on } \hat{\mathbf{s}}\cdot\hat{z}<0. \tag{II.6}$$

Here, $r_2(\hat{\mathbf{s}}_2\to\hat{\mathbf{s}})$ denotes the Fresnel reflectio coefficien for light incident on the $z = z_0$ boundary from within the slab in direction $\hat{\mathbf{s}}_2$ with $\hat{\mathbf{s}}_2\cdot\hat{z} > 0$ as governed by Snell's law.

Upon solution of the boundary value problem consisting of Eq. (II.1) subject to boundary conditions (II.4) and (II.6), we obtain $I(\hat{\mathbf{s}},x,y,z)$. To study the transmission of this beam, we compute the transmittance, $T(x,y)$, define as

$$T(x,y) = \int_{\hat{\mathbf{s}}\cdot\hat{z}>0} t_2(\hat{\mathbf{s}}'\to\hat{\mathbf{s}})I(\hat{\mathbf{s}}',x,y,z_0)\hat{\mathbf{s}}\cdot\hat{z}\mathrm{d}\hat{\mathbf{s}}. \tag{II.7}$$

Here, $t_2(\hat{\mathbf{s}}'\to\hat{\mathbf{s}})$ is the Fresnel transmission coefficien for light incident on the $z = z_0$ boundary from within the slab in direction $\hat{\mathbf{s}}'$ with $\hat{\mathbf{s}}'\cdot\hat{z} > 0$ transmitted in direction $\hat{\mathbf{s}}$ as governed by Snell's law.

In fact, we show in the results that follow the diffuse transmittance, T_d. The diffuse transmittance is define by Eq. (II.7) with I replaced by the diffuse intensity I_d. We describe the decomposition of I in terms of the reduced intensity I_{ri} and the diffuse intensity I_d in the Appendix.

III. THE ONE-WAY RADIATIVE TRANSFER EQUATION

Let $\mu = \cos\theta$ denote the cosine of the polar angle and φ denote the azimuthal angle. Then Eq. (II.1) can be written in terms of μ and φ as

$$\mu\partial_z I + \sqrt{1-\mu^2}(\cos\varphi\partial_x I + \sin\varphi\partial_y I) + I = \varpi_0\int_0^{2\pi}\int_{-1}^{1} p(\mu,\mu',\varphi-\varphi')I(\mu',\varphi',x,y,z)\mathrm{d}\mu'\mathrm{d}\varphi'. \tag{III.1}$$

Boundary condition (II.4) becomes

$$I(\mu,\varphi,x,y,0) = t_1(\hat{z})\frac{\delta(\mu-1)}{2\pi}b(x,y) + r_1(\mu)I(-\mu,\varphi,x,y,0) \quad \text{on } 0<\mu\le 1. \tag{III.2}$$

Boundary condition (II.6) becomes

$$I(\mu,\varphi,x,y,z_0) = r_2(\mu)I(-\mu,\varphi,x,y,z_0) \quad \text{on } -1\le\mu<0. \tag{III.3}$$

Note that we have incorporated Snell's law explicitly in boundary conditions (III.2) and (III.3).

A. Deriving the one-way RTE

We now introduce the forward and backward half-range diffuse intensities, define respectively as

$$I^{\pm} = I(\pm\mu,\varphi,x,y,z) \quad \text{for } 0<\mu\le 1\,. \tag{III.4}$$

It follows from Eq. (III.1) that $I^{\pm}$ satisfy two coupled RTEs,

$$\pm\mu\partial_z I^{\pm} + \sqrt{1-\mu^2}(\cos\varphi\partial_x I^{\pm} + \sin\varphi\partial_y I^{\pm}) + I^{\pm} = \varpi_0\mathscr{P}_f I^{\pm} + \varpi_0\mathscr{P}_b I^{\mp}. \tag{III.5}$$

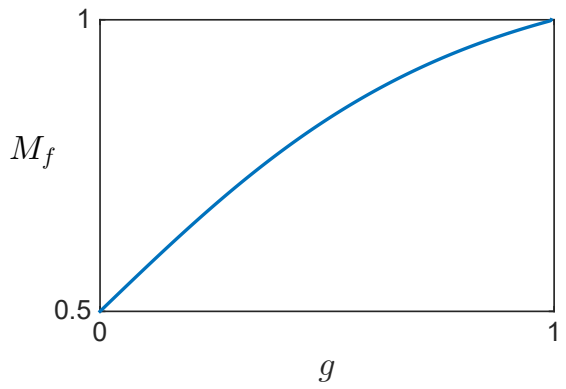

FIG. 1. (color online) The mass contained in the forward hemisphere of the Henyey-Greenstein scattering phase function (II.2) [see Eq. (III.9).]

Here,

$$\mathscr{P}_{f,b} = \int_0^{2\pi}\int_0^1 p_{f,b}(\mu,\mu',\varphi-\varphi')[\cdot]\mathrm{d}\mu'\mathrm{d}\varphi' \tag{III.6}$$

with p_f and p_b denoting the forward and backward scattering phase functions, respectively, which are restrictions of the original scattering phase function, *i*.e., $p_f = p(\mu,\mu',\varphi-\varphi') = p(-\mu,-\mu',\varphi-\varphi')$ and $p_b = p(\mu,-\mu,\varphi-\varphi') = p(-\mu,\mu',\varphi-\varphi')$ for $0<\mu,\mu'\le 1$. Note that the two equations in (III.5) are coupled because $I^{\mp}$ appears on the right-hand side. In terms of $I^{\pm}$, boundary condition (III.2) is given as

$$I^+(\mu,\varphi,x,y,0) = t_1(\hat{z})\frac{\delta(\mu-1)}{2\pi}b(x,y) + r_1(\mu)I^-(\mu,\varphi,x,y,0), \tag{III.7}$$

and boundary condition (III.3) is given as

$$I^-(\mu,\varphi,x,y,z_0) = r_2(\mu)I^+(\mu,\varphi,x,y,z_0). \tag{III.8}$$

Both boundary conditions (III.7) and (III.8) are on $0<\mu\le 1$. The boundary value problem comprised of Eq. (III.5) subject to boundary conditions (III.7) and (III.8) is equivalent to the boundary value problem for the RTE given above.

Now we consider anisotropic scattering which is forward peaked. Because of the normalization given in Eq. (II.3), the "mass" contained in the forward hemisphere, $\hat{\mathbf{s}}\cdot\hat{z}>0$ is define as

$$M_f = \int_{\hat{\mathbf{s}}'\cdot\hat{z}>0} p(\hat{z}\cdot\hat{\mathbf{s}}')\mathrm{d}\hat{\mathbf{s}}' = 2\pi\int_0^1 p(\xi)\mathrm{d}\xi. \tag{III.9}$$

For isotropic scattering with $g=0$, $M_f = 1/2$. For purely forward scattering with $g=1$, $M_f = 1$. For the Henyey-Greenstein scattering phase function given in Eq. (II.2), we plot M_f for $0\le g\le 1$ in Fig. 1.

Notice in Fig. 1 that for $g>0.65$ that M_f contains over 90% of the total mass. Therefore, it follows that for these values of g that $\|\mathscr{P}_f I^{\pm}\| \gg \|\mathscr{P}_b I^{\mp}\|$. In light of this observation, we neglect the $\mathscr{P}_b I^-$ term in Eq. (III.5), and fin that I^+ satisfie

$$\mu\partial_z I^+ + \sqrt{1-\mu^2}(\cos\varphi\partial_x I^+ + \sin\varphi\partial_y I^+) + I^+ = \varpi_0\mathscr{P}_f I^+. \tag{III.10}$$

We call Eq. (III.10) the *one-way RTE*, because it describes the (approximate) behavior of I^+. Notice that I^- does not appear at all in Eq. (III.10). Consequently, by neglecting the second term in boundary condition (III.7), we obtain the "initial" condition,

$$I^+(\mu,\varphi,x,y,0) = t_1(\hat{z})\frac{\delta(\mu-1)}{2\pi}b(x,y) \quad \text{on } 0<\mu\le 1. \tag{III.11}$$

Upon solution of this initial value problem, we compute the transmittance through the slab through evaluation of

$$T(x,y) = \int_0^{2\pi}\int_0^1 t_2(\mu'\to\mu)I^+(\mu',\varphi,x,y,z_0)\mu\mathrm{d}\mu\mathrm{d}\varphi. \tag{III.12}$$

B. Connecting the one-way RTE to the RTE

In fact, we can consider the initial value problem comprised of Eq. (III.10) subject to initial condition (III.12) to be the firs iteration of the following iteration scheme for solving the coupled system (III.5).

1. Set $I^{(0)-}=0$ (corresponding to $n=0$) and $n=1$.
2. Solve the initial value problem for the forward propagating radiance

$$\mu\partial_z I^{(n)+} + \sqrt{1-\mu^2}(\cos\varphi\partial_x I^{(n)+} + \sin\varphi\partial_y I^{(n)+}) + I^{(n)+} - \varpi_0\mathscr{P}_f I^{(n)+} = \varpi_0\mathscr{P}_b I^{(n-1)-},$$

   in $0<z\le z_0$ subject to

$$I^{(n)+}(\mu,\varphi,x,y,0) = t_1(\hat{z})\frac{\delta(\mu-1)}{2\pi}b(x,y) + r_1(\mu)I^{(n-1)-}(\mu,\varphi,x,y,0).$$

3. Solve the fina value problem for the backward propagating radiance

$$-\mu\partial_z I^{(n)-} + \sqrt{1-\mu^2}(\cos\varphi\partial_x I^{(n)-} + \sin\varphi\partial_y I^{(n)-}) + I^{(n)-} - \varpi_0\mathscr{P}_f I^{(n)-} = \varpi_0\mathscr{P}_b I^{(n)+}$$

   in $z_0>z\ge 0$ subject to

$$I^{(n)-}(\mu,\varphi,x,y,z_0) = r_2(\mu)I^{(n)+}(\mu,\varphi,x,y,z_0).$$

4. Repeat Steps 2 through 4 for $n\leftarrow n+1$ until convergence is reached.
5. The complete solution of the original RTE problem is given by Eq. (III.4).

In contrast to the conventional source iteration method [14] which computes the scattering integral over all directions, this iteration scheme is essentially the same as the improved source-iteration introduced by Gao and Zhao [15].

C. The reduced and diffuse intensities

The Appendix shows the decomposition of I into the reduced intensity, I_{ri}, and the diffuse intensity, I_d, for the RTE. This analysis leads to a nonhomogenous boundary value problem for I_d. Here, we decompose I^+ into the sum $I^+ = I^+_{ri} + I^+_d$ with I^+_{ri} denoting the reduced forward intensity, and I^+_d denoting the diffuse forward intensity.

The reduced forward intensity satisfie the initial value problem comprised of

$$\mu\partial_z I^+_{ri} + \sqrt{1-\mu^2}(\cos\varphi\partial_x I^+_{ri} + \sin\varphi\partial_y I^+_{ri}) + I^+_{ri} = 0, \quad \text{(III.13)}$$

subject to initial condition

$$I_{ri}(\mu,\varphi,x,y,0) = t_1(\hat{z})\frac{\delta(\mu-1)}{2\pi}b(x,y). \quad \text{(III.14)}$$

The solution of this initial value problem is given by

$$I_{ri}(\mu,\varphi,x,y,0) = t_1(\hat{z})\frac{\delta(\mu-1)}{2\pi}b(x,y)e^{-z}. \quad \text{(III.15)}$$

Using $I^+ = I^+_{ri} + I^+_d$ and substituting Eq. (III.15) into Eq. (III.10), we fin that I^+_d satisfie the nonhomogeneous problem

$$\mu\partial_z I^+_d + \sqrt{1-\mu^2}(\cos\varphi\partial_x I^+_d + \sin\varphi\partial_y I^+_d) + I^+_d = \varpi_0\mathscr{P}_f I^+_d + Q^+_{ri}, \quad \text{(III.16)}$$

with

$$Q^+_{ri} = \mathscr{P}_f I^+_{ri} = t_1(\hat{z})\varpi_0 p_f(\mu,1,\cdot)b(x,y)e^{-z}. \quad \text{(III.17)}$$

Additionally, we fin that I^+_d satisfie the homogeneous initial condition

$$I_d(\mu,\varphi,x,y,0) = 0 \quad \text{on } 0<\mu\le 1. \quad \text{(III.18)}$$

Upon solution of the initial value problem for I^+_d comprised of Eq. (III.16) subject to initial condition (III.18), we compute the one-way RTE approximation of the diffuse transmittance through evaluation of

$$T_d(x,y) = \int_0^{2\pi}\int_0^1 t_2(\mu'\to\mu)I^+_d(\mu',\varphi,x,y,z_0)\mu\mathrm{d}\mu\mathrm{d}\varphi. \quad \text{(III.19)}$$

IV. NUMERICAL METHOD

To solve the initial value problem for the one-way RTE consisting of Eq. (III.16) with initial condition (III.18), we use the discrete ordinate method. This method follows closely the method described in [18], so we give only the main details here.

A. Transverse spatial Fourier transform

Let Ψ denote the Fourier tranform

$$\Psi = \iint I^+_{\mathrm{d}}(\mu,\varphi,x,y,z) \times \exp[-\mathrm{i}k(x\cos\phi + y\sin\phi)]\mathrm{d}x\mathrm{d}y. \quad \text{(IV.1)}$$

Here, k and ϕ are the polar coordinates of the transform space. By transforming Eq. (III.10), we obtain

$$\mu\partial_z\Psi + \mathrm{i}k\sqrt{1-\mu^2}\cos\bar{\varphi}\Psi + \Psi = \varpi_0\mathscr{P}_f\Psi + q(\mu)e^{-z}, \quad \text{(IV.2)}$$

with $\bar{\varphi} = \phi - \varphi$, and

$$q(\mu) = t_1(\hat{z})\varpi_0 P_0 p(\mu,1,\cdot)\exp(-k^2R^2/8)e^{-z}. \quad \text{(IV.3)}$$

Transforming Eq. (III.18) yields

$$\Psi|_{z=0} = 0. \quad \text{(IV.4)}$$

Because Ψ is 2π-periodic in φ and ϕ, $\mathscr{P}_f$ is invariant with respect to rotations in φ, and Eq. (IV.4) is independent of φ, Ψ depends only on the relative angle $\bar{\varphi}$.

B. Discrete ordinate method

Let μ_m and w_m for $m = 1,\cdots,M$ denote the M-point Gauss-Legendre quadrature abscissas and weights corresponding to Gauss-Legendre quadrature rule:

$$\int_{-1}^1 f(\mu)\mathrm{d}\mu \approx \sum_{m=1}^M f(\mu_m)w_m. \quad \text{(IV.5)}$$

For convenience, we introduce $\tilde{\mu}_m = (\mu_m+1)/2$ and $\tilde{w}_m = w_m/2$, so that Gauss-Legendre quadrature rule for an integral over the half-range, $0<\mu\le 1$, is

$$\int_0^1 f(\mu)\mathrm{d}\mu \approx \sum_{m=1}^M f(\tilde{\mu}_m)\tilde{w}_m. \quad \text{(IV.6)}$$

Let $\bar{\varphi}_n = \pi(n-1)/N$ for $n = 1,\cdots,2N$. We introduce the discretized forward scattering operator

$$P^{MN}_f\Psi(\mu,\bar{\varphi},k,z) = \frac{\pi}{N}\sum_{n'=1}^{2N}\sum_{m'=1}^{M} p_f(\mu,\tilde{\mu}_{m'},\bar{\varphi}-\bar{\varphi}_{n'}) \times \Psi(\tilde{\mu}_{m'},\bar{\varphi}_{n'},k,z)\tilde{w}_{m'}. \quad \text{(IV.7)}$$

We now replace $\mathscr{P}_f$ by P^{MN}_f in Eq. (IV.2) and evaluate that result at μ_m and φ_n which yields

$$\tilde{\mu}_m\partial_z\Psi_{mn} + \mathrm{i}k\sqrt{1-\tilde{\mu}_m^2}\cos\bar{\varphi}_n\Psi_{mn} + \Psi_{mn} = \varpi_0 P^{MN}_f\Psi_{mn} + q_m e^{-z}, \quad \text{(IV.8)}$$

for $m = 1,\cdots,M$ and $n = 1,\cdots,2N$. Here, $\Psi_{mn}(k,z)$ denotes the approximation of $\Psi(\tilde{\mu}_m,\bar{\varphi}_n,k,z)$, and $q_m = q(\mu_m)$.

We represent the solution of Eq. (IV.8) as the sum $\Psi_{mn} = \Psi^H_{mn} + \Psi^P_{mn}$ where Ψ^H_{mn} is the homogeneous solution and Ψ^P_{mn} is the particular solution. The particular solution is given by $\Psi^P_{mn} = \psi_{mn} e^{-z}$ where ψ_{mn} satisfie the linear system

$$\left[-\tilde{\mu}_m + \mathrm{i}k\sqrt{1-\tilde{\mu}_m^2}\cos\bar{\varphi}_n - \varpi_0 P_f^{MN}\right]\psi_{mn} = q_m, \quad \text{(IV.9)}$$

for $m = 1,\cdots,M$ and $n = 1,\cdots,2M$. The homogeneous solution is given by $\Psi_{mn} = V_{mn}e^{\lambda z}$ where the pair λ, and V_{mn} satisfie the following generalized eigenvalue problem

$$\lambda\tilde{\mu}_m V_{mn} + \mathrm{i}k\sqrt{1-\tilde{\mu}_m^2}\cos\bar{\varphi}_n V_{mn} + V_{mn} = \varpi_0 P_f^{MN} V_{mn}, \quad \text{(IV.10)}$$

for $m = 1,\cdots,M$ and $n = 1,\cdots,2N$. There are $2MN$ eigenvalues that we index as λ_j for $j = 1,\cdots,2MN$ with corresponding eigenvectors $V^{(j)}_{mn}$. For $0 < \varpi_0 < 1$, all eigenvalues lie on the left-half of the complex plane. Consequently, the general solution of Eq. (IV.8) is given by

$$\Psi_{mn} = \sum_{j=1}^{2MN} V^{(j)}_{mn} e^{\lambda_j z} c_j + \psi_{mn} e^{-z}, \quad \text{(IV.11)}$$

for $m = 1,\cdots,M$ and $n = 1,\cdots,2N$ with the set of expansion coefficients $\{c_j\}$, to be determined. We determine this expansion coefficient by imposing initial condition (IV.4) at each of the discrete ordinates leading to the linear system

$$\sum_{j=1}^{2MN} V^{(j)}_{mn} c_j + \psi_{mn} = 0, \quad \text{(IV.12)}$$

for $m = 1,\cdots,M$ and $n = 1,\cdots 2N$.

C. Quasi-fast Hankel transform

In terms of Ψ, the solution I^+ is given by the inverse transform

$$I^+(\mu,\varphi,x,y,z) = (2\pi)^{-2}\int_0^\infty\int_0^{2\pi}\Psi(\mu,\varphi-\phi,k,z) \times \exp[\mathrm{i}k(x\cos\phi + y\sin\phi)]\mathrm{d}\phi k\mathrm{d}k. \quad \text{(IV.13)}$$

Substituting this expression into Eq. (III.12), we fin that the diffuse transmittance is given by the Hankel transform,

$$T(\rho) = (2\pi)^{-1}\int_0^\infty \bar{\Psi}(k,z_0) J_0(k\rho) k\mathrm{d}k, \quad \text{(IV.14)}$$

with $\rho^2 = x^2 + y^2$, and

$$\bar{\Psi}(k,z_0) = \int_0^{2\pi}\int_0^1 \Psi(\mu,\bar{\varphi},k,z_0)\mu\mathrm{d}\mu\mathrm{d}\bar{\varphi}. \quad \text{(IV.15)}$$

We approximate $\bar{\Psi}(k,z)$ using the solution given in Eq. (IV.12), and using the product quadrature rule to obtain

$$\bar{\Psi}(k,z_0) \approx \frac{\pi}{N}\sum_{n=1}^{2N}\sum_{m=1}^{M}\Psi_{mn}(k,z_0)\tilde{\mu}_m\tilde{w}_m. \quad \text{(IV.16)}$$

To compute Eq. (IV.14), we sample $\bar{\Psi}(k,z_0)$ at a discrete set of k values evenly spaced in $\log k$ since even spacing in $\log k$ converts the Hankel transform to a discrete Fourier convolution [19]. For the results shown below, we have used a Matlab implementation of the quasi-fast Hankel transform [20].

V. NUMERICAL RESULTS

To evaluate the accuracy and effica y of the one-way RTE to compute the diffuse transmittance, we compare numerical solutions of it with those computed using Monte Carlo simulations of the RTE. For the Monte Carlo simulations, we have used the `MCML` [16] and `CONV` [17] codes. For all of the numerical results shown here, we have set the total power to $P_0 = 1$ and the beam radius to $R = 0.5$. We have used 10^7 photons for each of the Monte Carlo simulations results we show below. We have used $M = 16$ for all of the one-way RTE calculations except for when $g = 0.95$ where we have used $M = 32$. In what follows, we evaluate comparisons as we vary (i) the anisotropy factor, g, (ii) the single scattering albedo, ϖ_0, and the optical thickness z_0.

A. Anisotropy factor

To study the one-way RTE as the anisotropy factor, g, varies, we study the diffuse transmittance with $\varpi_0 = 0.9$ and $z_0 = 2$. Figure 2 shows comparisons of the diffuse transmittance for $g = 0.75$, 0.85, and 0.95. The x-axis is the radial coordinate, $\rho = \sqrt{x^2+y^2}$. In each of these results, we fin that the one-way RTE accurately approximates the Monte Carlo results. When $g = 0.95$, the results are indistinguishable.

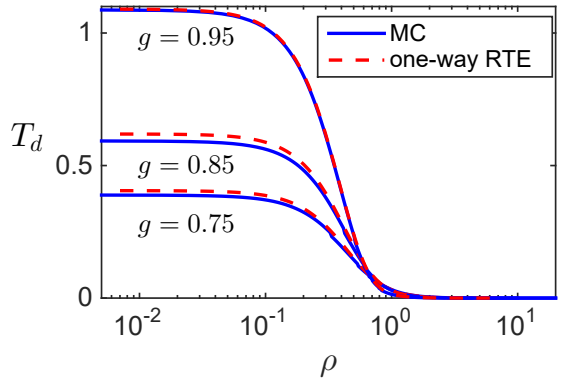

FIG. 2. (color online) Comparisons of the diffuse transmittance computed using Monte Carlo simulations of the RTE (solid curves) and the one-way RTE (dashed curves) as a function of the radial coordinate ρ (log scale) for varying anisotropy factors: $g = 0.75$, 0.85, and 0.95. Here, $\varpi_0 = 0.9$ and $z_0 = 2$.

B. Single scattering albedo

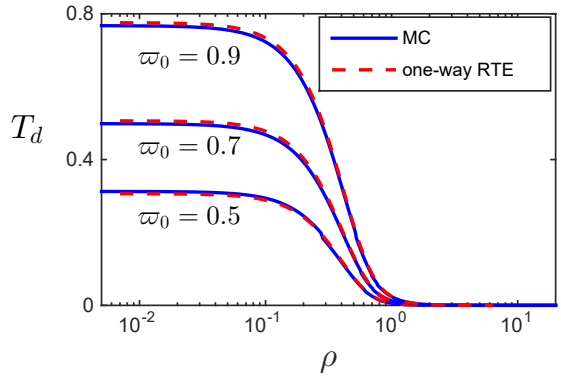

FIG. 3. (color online) Same as Fig. 2, but for varying albedo, ϖ_0 = 0.5, 0.7, and 0.9. Here, $g = 0.9$ and $z_0 = 2$.

To study the one-way RTE as the single scattering albedo, ϖ_0, varies, we study the diffuse transmittance with $g = 0.9$ and $z_0 = 2$. Figure 3 shows comparisons of the diffuse transmittance for $\varpi_0 = 0.5$, 0.7, and 0.9. In each of these results, we fin that the one-way RTE accurately approximates the Monte Carlo results.

C. Optical thickness

To study the one-way RTE as the optical thickness, z_0, varies, we study the diffuse transmittance with $\varpi_0 = 0.9$ and $g = 0.9$. Figure 4 shows comparisons of the diffuse transmittance for $z_0 = 2$, 5, and 10. In each of these results, we fin that the one-way RTE accurately approximates the Monte Carlo results.

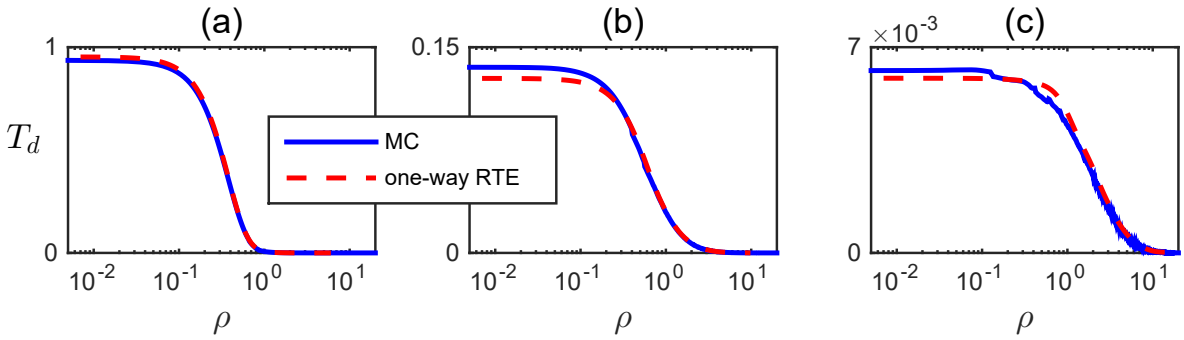

FIG. 4. (color online) Same as Fig. 2, but for varying thickness, (a) $z_0 = 2$, (b) $z_0 = 5$, and (c) $z_0 = 10$. Here $\varpi_0 = 0.9$ and $g = 0.9$.

D. Refractive index

We study the one-way RTE as the relative refractive index m varies. Here, m is define as the ratio of the refractive index inside the slab over that outside of the slab **Is it standard to use m instead of n?** In particular, we study the diffuse transmittance with $\varpi_0 = 0.9$, $g = 0.9$ and $z_0 = 2$. Figure 5 shows comparisons of the diffuse transmittance for $m = 1.0$, 1.2, and 1.4. In each of these results, we fin that the one-way RTE accurately approximates the Monte Carlo results.

VI. CONCLUSIONS

To study the transmission of a beam in a forward-peaked scattering medium, we have introduced the one-way RTE. This approximation results from neglecting backscattering. Rather than solving a boundary value problem, the one-way RTE requires only the prescription of "initial data" at the boundary on which light is incident. This difference leads to a major conceptual simplificatio in computing the diffuse transmittance. The one-way RTE can be thought of as the firs iteration in a more effective iterative scheme to solve the

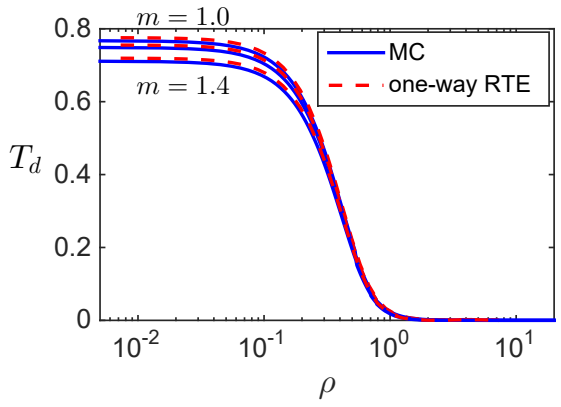

FIG. 5. (color online) Same as Fig. 2, but for varying refractive index mismatch, $m = 1.0$, 1.2, and 1.4. Here, $\varpi_0 = 0.9$, $g = 0.9$, and $z_0 = 2$.

full RTE. Our numerical results show that the one-way RTE effectively approximates the diffuse transmittance of a Gaussian beam incident on a slab composed of a uniform absorbing and scattering medium. It does so even for moderately large anisotropy factors over a broad range of single scattering albedo values and optical thicknesses. Therefore, it should be useful for a diverse array of applications. Because of its simplicity and demonstrated effectiveness, the one-way radiative transfer equation should be a very useful for studying the transmission of light in anisotropy scattering media.

APPENDIX: THE REDUCED AND DIFFUSE INTENSITIES FOR THE RTE

We write the intensity as the sum $I = I_{ri} + I_d$ where I_{ri} denotes the reduced intensity and I_d denotes the diffuse intensity. The reduced intensity satisfie

$$\hat{\mathbf{s}}\cdot\nabla I_{ri} + I_{ri} = 0, \tag{A1}$$

subject to boundary conditions

$$I_{ri}(\hat{\mathbf{s}},x,y,0) = t_1(\hat{z})\delta(\hat{\mathbf{s}}-\hat{z})\frac{2P_0}{\pi R^2}\exp\left[-2\left(\frac{x^2+y^2}{R^2}\right)\right] + r_1(\hat{\mathbf{s}}_1\to\hat{\mathbf{s}})I_{ri}(\hat{\mathbf{s}}_1,x,y,0) \quad \text{on } \hat{\mathbf{s}}\cdot\hat{z}>0, \tag{A2}$$

and

$$I_{ri}(\hat{\mathbf{s}},x,y,z_0) = r_2(\hat{\mathbf{s}}_2\to\hat{\mathbf{s}})I_{ri}(\hat{\mathbf{s}}_2,x,y,z_0) \quad \text{on } \hat{\mathbf{s}}\cdot\hat{z}<0. \tag{A3}$$

The boundary value problem comprised of Eq. (A1) subject to boundary conditions (A2) and (A3) is easily solved. However, the result is an overly complex expression for the purposes here. Instead, we use the following approximation

$$I_{ri}(\hat{\mathbf{s}},\rho,z) \approx t_1(\hat{z})\frac{2P_0}{\pi R^2}\exp(-2\rho^2/R^2) \times \begin{cases} \dfrac{r_2(\hat{z}\to-\hat{z})\delta(\hat{\mathbf{s}}+\hat{z})e^{z-z_0}}{1-r_1(-\hat{z}\to\hat{z})r_2(\hat{z}\to-\hat{z})e^{-2z_0}}, & \hat{\mathbf{s}}\cdot\hat{z}<0, \\ \dfrac{\delta(\hat{\mathbf{s}}-\hat{z})e^{-z}}{1-r_1(-\hat{z}\to\hat{z})r_2(\hat{z}\to-\hat{z})e^{-2z_0}}, & \hat{\mathbf{s}}\cdot\hat{z}>0. \end{cases} \tag{A4}$$

This approximation is suggested by Ishimaru [2] (see Chapter 8, Section 3). It satisfie boundary conditions (A2) and (A3), but approximately satisfie Eq. (A1).

Substituting Eq. (A4) into Eq. (II.1) using $I = I_{ri} + I_d$, we fin that I_d satisfie the nonhomogeneous RTE,

$$\hat{\mathbf{s}}\cdot\nabla I_d + I_d - \varpi_0\int_{\mathbb{S}^2} p(\hat{\mathbf{s}}\cdot\hat{\mathbf{s}}')I_d(\hat{\mathbf{s}}',\mathbf{r})\mathrm{d}\hat{\mathbf{s}}' = Q_{ri}^- + Q_{ri}^+, \tag{A5}$$

with

$$Q_{ri}^- = \frac{\varpi_0 t_1(\hat{z})r_2(\hat{z}\to-\hat{z})p(\hat{\mathbf{s}}\cdot-\hat{z})}{1-r_1(-\hat{z}\to\hat{z})r_2(\hat{z}\to-\hat{z})e^{-2z_0}} \times\frac{2P_0}{\pi R^2}\exp(-2\rho^2/R^2+z-z_0), \tag{A6}$$

and

$$Q_{ri}^+ = \frac{\varpi_0 t_1(\hat{z})p(\hat{\mathbf{s}}\cdot\hat{z})}{1-r_1(-\hat{z}\to\hat{z})r_2(\hat{z}\to-\hat{z})e^{-2z_0}} \times\frac{2P_0}{\pi R^2}\exp(-2\rho^2/R^2-z). \tag{A7}$$

The boundary conditions for Eq. (A5) are

$$I_d(\hat{\mathbf{s}},x,y,0) = r_1(\hat{\mathbf{s}}_1\to\hat{\mathbf{s}})I_d(\hat{\mathbf{s}}_1,x,y,0) \quad \text{on } \hat{\mathbf{s}}\cdot\hat{z}>0, \tag{A8}$$

and

$$I_d(\hat{\mathbf{s}},x,y,z_0) = r_2(\hat{\mathbf{s}}_2\to\hat{\mathbf{s}})I_d(\hat{\mathbf{s}}_2,x,y,z_0) \quad \text{on } \hat{\mathbf{s}}\cdot\hat{z}<0. \tag{A9}$$

Upon solution of the boundary value problem comprised of Eq. (A5) subject to boundary conditions (A8) and (A9), we compute the diffuse transmittance,

$$T_d(x,y) = \int_{\hat{\mathbf{s}}\cdot\hat{z}>0} t_2(\hat{\mathbf{s}}'\to\hat{\mathbf{s}})I_d(\hat{\mathbf{s}}',x,y,z_0)\hat{\mathbf{s}}\cdot\hat{z}\mathrm{d}\hat{\mathbf{s}}. \tag{A10}$$

[1] S. Chandrasekhar, *Radiative Transfer* (Dover, 1960).
[2] A. Ishimaru, *Wave Propagation and Scattering in Random Media* (IEEE Press, 1999).
[3] G. Thomas and K. Stamnes, *Radiative Transfer in the Atmosphere and Ocean* (Cambridge University Press, 2002).
[4] A. Marshak and A. Davis, *3D Radiative Transfer in Cloudy Atmospheres* (Springer, 2005).
[5] L.-H. Wang and H. Wu, *Biomedical Optics: Principles and Imaging* (Wiley, 2007).
[6] G. C. Pomraning, "The Fokker-Planck operator as an asymptotic limit," Math. Models Methods Appl. Sci. **2**, 21-36 (1992).
[7] E. W. Larsen, "The linear Boltzmann equation in optically thick systems with forward-peaked scattering," Prog. Nucl. Energy **34**, 413-423 (1999).

[8] G. C. Pomraning, "Higher order Fokker-Planck operators," Nucl. Sci. Eng. **124**, 390-397 (1996).
[9] A. K. Prinja and G. C. Pomraning, "A generalized Fokker-Planck model for transport of collimated beams," Nucl. Sci. Eng. **137**, 227-235 (2001).
[10] C. L. Leakeas and E. W. Larsen, "Generalized Fokker-Planck approximation of particle transport with highly forward-peaked scattering," Nucl. Sci. Eng. **137**, 236-250 (2001).
[11] P. González-Rodríguez and A. D. Kim, "Light propagation in tissues with forward-peaked and large-angle scattering," Appl. Opt. **47**, 2599-2609 (2008).
[12] A. D. Kim, "Correcting the diffusion approximation at the boundary," J. Opt. Soc. Am. A **28**, 1007-1015 (2011).
[13] E. Vitkin, V. Turzhitsky, L. Qiu, L. Guo, I. Itzkan, E. B. Hanlon, and L. T. Perelman, "Photon diffusion near the point-of-entry in anisotropically scattering turbid media," Nature Comm. **2**, 587 (2011).
[14] E. E. Lewis and W. F. Miller, Jr., *Computational Methods of Neutron Transport* (American Nuclear Society, 1993)
[15] H. Gao and H. Zhao, "A fast forward solver of radiative transfer equation," Transport Theory Statist. Phys. **38**, 149-192 (2009).
[16] L.-H. Wang, S. L. Jacques, and L.-Q. Zheng, "MCML - Monte Carlo modeling of photon transport in multi-layered tissues," Comput. Meth. Prog. Bio. **47**, 131-146 (1995).
[17] L.-H. Wang, S. L. Jacques, and L.-Q. Zheng, "CONV - Convolution for responses to a finit diameter photon beam incident on multi-layered tissues," Comput. Meth. Prog. Bio. **54**, 141-150 (1997).
[18] A. D. Kim and M. Moscoso, "Beam propagation in sharply peaked forward scattering media," J. Opt. Soc. Am. A **5**, 797-803 (2004).
[19] 12. A. E. Siegman, "Quasi-fast Hankel transform," Opt. Lett. **1**, 13-15 (1977).
[20] M. Leutenegger, "Hankel transform," (http://www.mathworks.com/matlabcentral/file xchange/13371-hankel-transform), MATLAB Central File Exchange. Retrieved November 26, 2013.